



Assessing the accuracy of hexagonal versus square tilled grids in preserving DEM surface flow directions

Luís de Sousa, Fernanda Nery, Ricardo Sousa and João Matos

Departamento de Engenharia Civil e Arquitectura
Instituto Superior Técnico (IST)
Avenida Rovisco Pais
1049-001 Lisbon, Portugal
Tel. +351-218418350, Fax: +351-218419765
lads@mega.ist.utl.pt; nery@ist.utl.pt; rts@civil.ist.utl.pt; jmatos@civil.ist.utl.pt

Abstract

The theoretical advantages of hexagonal grids over rectangular grids have been known for a large number of years. Among these, two can be stressed out: the higher spatial resolution achieved with the same number of samples and the isotropy of local neighbourhoods. This work explores such advantages in the representation of flow directions used in hydrologic modeling. The 3 arc-second resolution DEM data collected by the Shuttle Radar Topography Mission (SRTM) was resampled to increasingly lower resolution grids, both of squares and hexagons. The flow direction vectors were computed in each of these grids using the steepest down slope neighbour criteria; for the hexagonal grids an equivalent model was used. Reference data was obtained from the original full resolution DEM, calculating the resulting flow direction vectors of the samples contained inside each of the lower resolution cells. The accuracy of each model in preserving the original DEM flow direction characteristics was assessed by comparing the angles defined by lower resolution flow vectors with the resulting vectors of the corresponding full resolution samples. In the data analysis phase, the influence of local terrain morphology and variability was evaluated. A set of tests were conducted in the Minho River basin (ca. 16950 Km² in the northwest of the Iberian Peninsula). The results obtained suggest a superior capacity of the hexagonally tilled grids in maintaining the original flow directions, as given by the resulting vector of the original samples.

Keywords: regular tessellation, hexagonal grid, flow direction

1 Introduction

Hexagonal tiles have long been known to be a better structure than squares tiles to continuously divide the bi-dimensional space. Hexagons yield a compacter division of space and an isotropic neighbourhood.

Each cell on a square grid has four neighbours with which shares an edge and another four with which shares a vertex. This kind of anisotropic relation allows for the definition of neighbourhood at least in two different fashions:

- 4-neighbourhood, including only the cells to which the central one shares an edge;
- 8-neighbourhood, including all the cells to which the central one shares an edge or a vertex.

The diagonal cells are at a larger distance to the central cell, as can be observed in Figure 1.

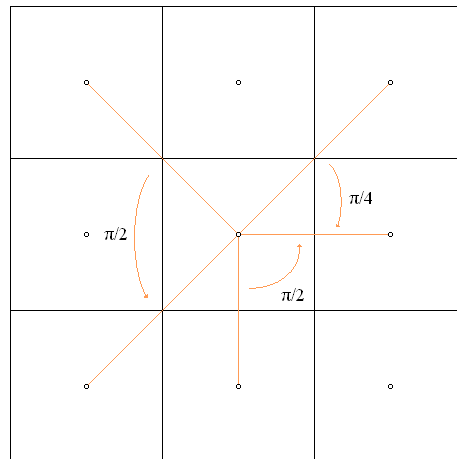


Figure 1 Neighbourhood relations on a square grid.

On a hexagonal grid there are no ambiguities in neighbourhood definitions, all six neighbours share an edge with the central cell, and are at the same distance from its center (Figure 2).

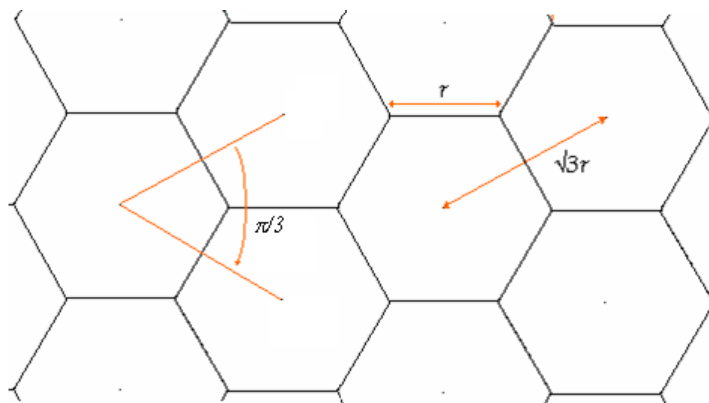


Figure 2 Neighbourhood relations on a hexagonal grid.

In the digital information systems field, work with hexagons dates back to decade of 1960, especially by the hand of Goolay [Goolay 1969] who investigated hexagonal sampling patterns applied to pattern recognition techniques. Goolay understood that these techniques are independent of the type of coordinate system, and so can be defined on a hexagonal sampling scheme the same way as on a square one. Furthermore, hexagons simplify the logic based on the nearest neighbour connectivity and in tandem the pattern transformations in binary images.

Ten years later, Mersereau presented arguably the most important work on the realm of hexagonal grids applied to the digital information systems [Mersereau, 1979]. Knowing that the mean sampling density is proportional to the area of sampling on the Fourier spectrum

Mersereau proved that a circular band-limited signal can be sampled by a hexagonal grid with 13.4% less samples than by a square grid. Figure 3 shows this difference: the square sampling scheme has to cover a larger area of the Fourier spectrum than the hexagonal sampling scheme, in order to fully rebuild the band-limited signal. A larger area covered in the Fourier spectrum results in a larger number of sampling points in space.

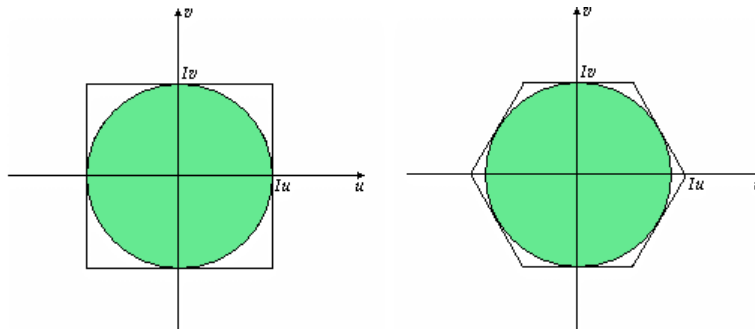


Figure 3 Area of the Fourier spectrum sampled in order to fully rebuild a circular band-limited signal (left, square sampling scheme; right, hexagonal sampling scheme).

From the work of Mersereau onwards others are worth mentioning: Frisch, Hasslacher and Pomeu [Frisch *et al.*, 1986] showed that hexagonally tiled cellular automata can evolve to reproduce the laws of flow dynamics, a property not found in square tiled automata. Hexagons have been proved a viable alternative in Digital Image Processing [Snyder *et al.*, 1999] and has a base for artificial vision systems, in this last case yielding the same or better results than square systems, without cost overheads [Stauton and Storey, 1989] [Stauton, 1989]. Hexagonal grids were also shown to be more efficient in representing linear elements than its square counterparts [Brimkov and Barneva, 2001].

Today the Environmental Monitoring and Assessment Program (EMAP) from the Environmental Protection Agency (EPA) of the United States advises as sampling scheme on the field a discrete global grid known as ISEAG (Icosahedral Snyder Equal Area Grid) which is an hexagonal grid with twelve singularities that are pentagons [Sahr *et al.*, 2003]. This kind of global grids tackles the distortions introduced in traditional global square grids based on cylindrical cartographic projections [Sahr and White, 1998].

But not all are advantages for hexagons, a hexagon cannot be divided in smaller hexagons, like can be done with squares. Still hexagons can be grouped in seven hexagons figures that yield the same neighbourhood properties of hexagons, like shown in Figure 4 [Lundmark *et al.*, 1999].

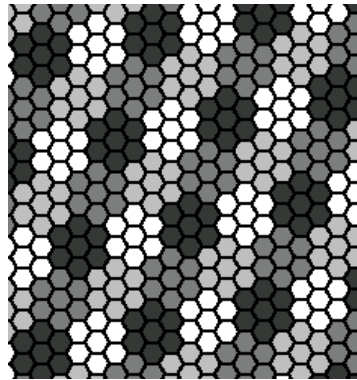


Figure 4 Super-hexagons built with seven hexagons.

2 Flow directions

Hydrologic modeling with Digital Elevation Models (DEM) always starts with the determination of water flow directions from each grid cell. Traditionally this is obtained using the algorithm proposed by O'Callaghan and Mark [O'Callaghan and Mark, 1984], known as D-8, in which the flow direction from a given cell is the direction of steepest descend to an immediate neighbour. This technique has some drawbacks in traditional square grids [Tarboton, 1997], and other models have been proposed where flow is considered to more than one neighbour, in order to reproduce more accurately the Hortonian flow paths observed in nature [Endreny and Wood, 2001][Endreny and Wood, 2003].

Despite its limitations, the D-8 model remains the most widely used flow direction coding system for DEM grids. Hence, D-8 algorithm was used in this work (partly because a clearly superior alternative hasn't yet emerged). The implementation of the D-6 counterpart in hexagonal grids is quite simple to devise: as all neighbours stand at the same distance from the center cell, the flow direction is simply the one of the neighbour with the lowest elevation value. Note that with a hexagonal grid only six different flow vectors can be coded in each cell, each of these vectors separated by an angle of $\pi/3$ radians. With a square grid eight different directions can be coded each with $\pi/4$ radians apart.

3 Data

In order to assess the performance of hexagonal grids in determining flow vectors a comparison was made against square grids of the same spatial resolution (cells with the same area).

The topographic data were derived from the DEM resultant from the Shuttle Radar Topography Mission (SRTM). These DEM are publicly available with a spatial resolution of 3 arc seconds covering about 70% of the planet's area. The DEM were projected using a Lambert Projection (which bears no area distortions) using the ellipsoid of the World Geodetic System (WGS84), with its central point on 2° 30' West and 40° North. The SRTM data are prone to errors resulting from Radar acquisition, namely the absence of return signal in large water bodies and noisy response in the oceans. Ocean areas were masked out of the DEM, using ancillary 1:25000 scale coastline vector data. The null elevation values in water bodies, due to lack of radar signal, were estimated using a raster adaptation of the second order interpolation algorithm proposed for the treatment of level triangles in TIN models by Zhu [Zhu *et al.*, 2001], according to the algorithms described in [de Sousa *et al.*, 2006].

The tests were conducted on the Minho (Miño) river watershed, located on the northern border of Portugal with Galicia, covering an area of 16 950 km². This particular watershed is interesting given its relatively large dimension and its morphology, which is mountainous to the East and with vast flatlands near the coastline.

The original DEM used for the test encompasses entirely the known watershed of the Minho River in a span of 2854 by 2235 square 90-meters cells.

4 Interpolating test grids

A set of DEM with diminishing spatial resolution was produced from the original grid. For each of the lower spatial resolutions, two new grids were created, one of hexagons and one of squares. These grids were obtained by averaging the values of the original full resolution grid in the neighbourhood of the center of each cell in the new grid. Although practical and simple this interpolation technique has the property of applying a low-pass filter to the original signal.

The chosen resolutions for testing were 30, 27, 24, 21, 18, 15, 12, 9 and 6 per cent of the original number of cells for the square grids and its equivalent for the hexagonal grids (Table 1). Note that the hexagonally tiled grids have less 13.4% cells than their square tiles counterparts.

Table 1 Test grids dimensions.

Resolution (fraction of original)	Nº cells Squares	Nº cells Hexagons	Square cell area (m ²)	Hexagon cell area (m ²)
0.30	574376	504855	90000	102150.0
0.27	464913	407925	111111	126111.1
0.24	367160	323856	140625	159609.4
0.21	280931	247036	183673	208469.4
0.18	206628	180950	250000	283750.0
0.15	143380	126283	360000	408600.0
0.12	91656	80730	562500	638437.5
0.09	51657	45325	1000000	1135000.0
0.06	22914	20414	2250000	2553750.0

This sequence of spatial resolutions was chosen by two main reasons:

- First of all for being multiples of 3, which avoids the interpolation becoming a cell aggregation process in the square case;
- Above this interval there are no major differences between square and hexagonal grids, and below this the interpolation degrades in excess the original DEM.

5 Process of test

The D-8 flow direction was determined for each cell of the original full resolution grid. Then for each grid of degraded resolution set, the resulting flow vector was computed. This was achieved by determining which original resolution cells have their center inside a given degraded resolution cell, and thus calculating the resulting flow vector (Figure 5). Beside this “averaged flow direction vector”, the simple D-8 and D-6 flow direction vectors were also calculated directly upon each of the lower resolution square and hexagonal grids (Figures 8 through 10).

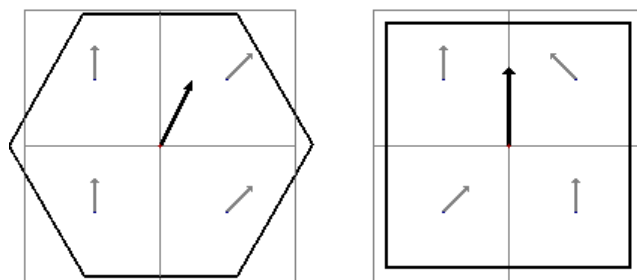


Figure 5 Resulting flow direction for the lower resolution cells.

6 Results

For each cell of each degraded resolution grid the angular difference between the two flow vectors explained above was computed. Then for each grid the mean angular error was calculated and also the number of cells in which the angular difference was greater than zero. These results are reunited in Table 2.

Table 2 Results.

Resolution (fraction of original)	Mean Angular difference (rad)		Number of errors	
	Squares	Hexagons	Squares	Hexagons
0.30	0.669	0.499	528047	462989
0.27	0.689	0.515	427355	374451
0.24	0.708	0.533	337665	296016
0.21	0.730	0.551	258183	225853
0.18	0.753	0.573	189320	165528
0.15	0.779	0.595	131376	114990
0.12	0.808	0.629	83791	73077
0.09	0.839	0.667	46897	41148
0.06	1.623	0.713	4726	18172

The angular difference is consistently lower for the hexagonal grids; as for the number of cells with differences, hexagonal grids yield lower values which can be explained by the also lower number of cells these grids have (Figures 6 and 7).

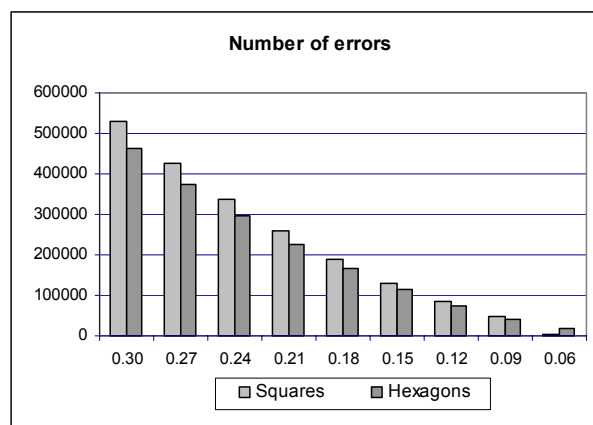


Figure 6 Number of errors in each test grid.

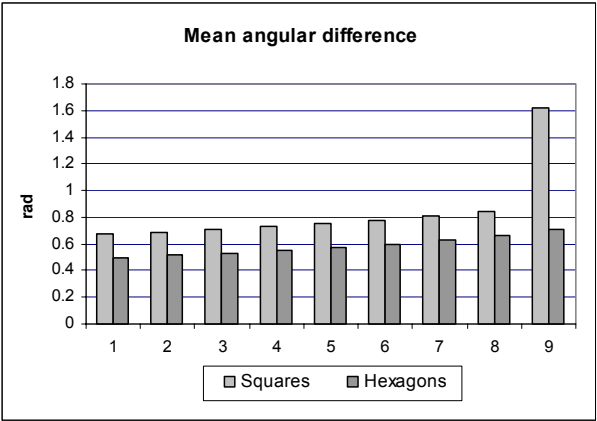


Figure 7 Mean angular difference from the test grids to the resulting flow grids.

7 Conclusions

Given the above results, it can be concluded that hexagonally tiled grids have better capacity in preserving original flow direction vectors when compared to squarely tiled ones. The results are more significant when considering that hexagonal grids only allow for the coding of six different flow directions whereas square grids allow for the coding of eight.

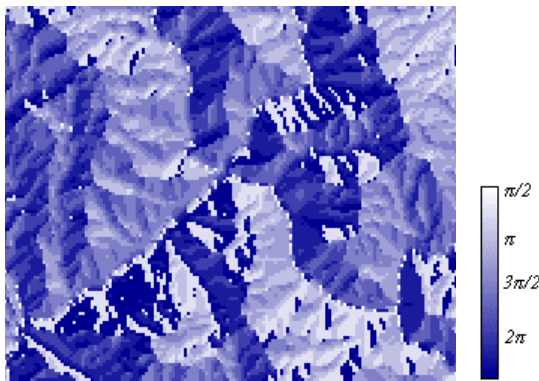


Figure 8 Detail of the original flow vector grid.

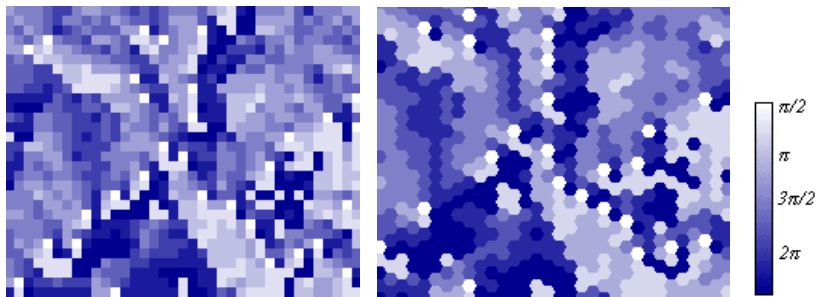


Figure 9 Detail of the 12% resolution test grids. Left, square tilled grid, right hexagon tilled grid.

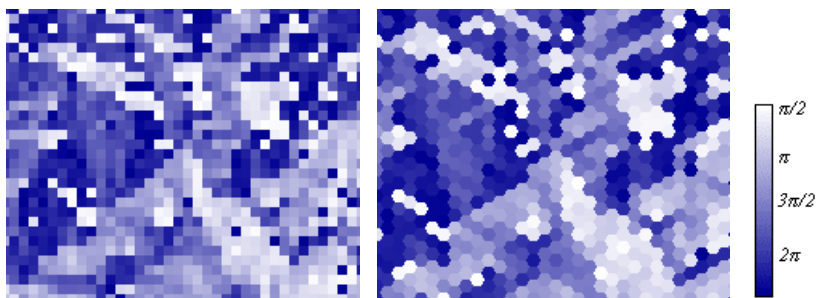


Figure 10 Detail of the 12% resolution resultant flow vector grids. Left, square tilled grid, right hexagon tilled grid.

References

- Brimkov, V. E. and Barneva, R. P., 2001, "Honeycomb" vs Square and Cubic Models, *Electronic Notes in Theoretical Computer Science*, 46.
- de Sousa, L., Nery, F. and Matos J., 2006, Metodologias de Processamento de dados SRTM para a produção de Modelos Digitais de Direcções de Escoamento, *VIII Congresso da Água*.
- Endreny, T. and Wood, F., 2001, Representing elevation uncertainty in runoff modeling and flowpath mapping, *Hydrologic Processes*, 15, 2223-2336.
- Endreny, T. and Wood, F., 2003, Maximizing spatial congruence of observed and DEM-delineated overland flow networks, *International Journal of Geographical Information Science*, vol. 17, no. 7, 699-713, Taylor & Francis.
- Frisch, U., Hasslacher, B. and Pomeu, Y., 1986, Lattice-Gas Automata for the Navier-Stokes Equation, *Physical Review Letters*, vol. 56, no. 14, pp1505-1508.
- Goolay, M., 1969, Hexagonal parallel pattern transformations, *IEEE Transactions on Computers*, vol. c-18, no. 8, pp733-740.
- Lundmark, A., Wadstromer, N., Li, H., 1999, Recursive subdivisions of the plane yielding nearly hexagonal regions, *RadioVetenskap och Kommunikation*.
- Mersereau, R. M., 1979, The processing of hexagonally sampled two-dimensional signals, *Proceedings of the IEEE*, 67, no. 6, pp930-949.
- O'Callaghan, J. and Mark, D., 1984, The extraction of drainage networks from digital elevation data, *Computer Vision Graphics Image Processes*, 28, 323-344.

- Sahr, K and White, D., 1998, Discrete Global Grid Systems, *Computing Science and Statistics*, 30, ed. S. Weisberg, Interface Foundation of North America, Inc., Fairfax Station, VA.
- Sahr, K., White, D., and Kimerling, A. J., 2003, Geodesic Discrete Global Grid Systems, *Cartography and Geographic Information Science*, vol. 30, no. 2, pp. 121-134.
- Snyder, W., Qi, H., and Sander, W. 1999, A Coordinate System for Hexagonal Pixels, *SPIE*, San Diego.
- Stauton, R. C., and Storey, N., 1989, A comparison between square and hexagonal sampling methods for pipeline image processing, *Proc. SPIE*, Vol. 1194, pp. 142-151.
- Stauton, R. C., 1989, Hexagonal Image Sampling: A Practical Proposition, *Proc. SPIE*, vol. 1008, pp23-27.
- Tarboton D., 1997, A new method for the determination of flow directions and upslope areas in grid digital elevation models, *Water Resouces Res.*, 33(2), 309-319.
- Zhu, H., Eastman, J. R., Toledano, J., 2001, "Triangulated irregular network optimization from contour data using bridge and tunnel edge removal", *International Journal of Geographical Information Science*, Volume 15, Number 3, pag. 271 – 286, Taylor & Francis.